Supporting Information

Tseng and Prather 10.1073/pnas.1209002109

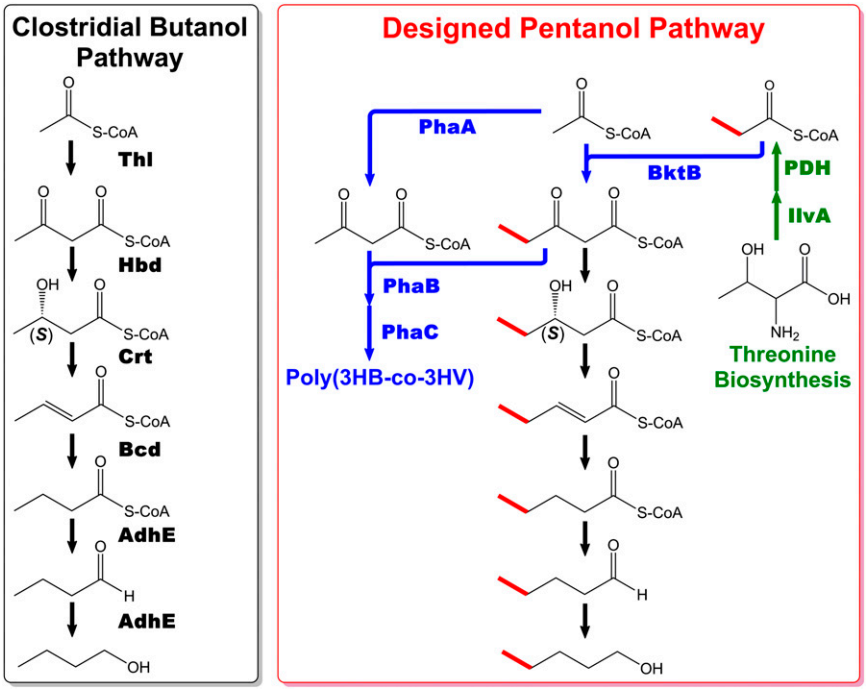

Fig. S1. Schematic of the butanol biosynthetic pathway (*Left*), poly(3HB-co-3HV) biosynthetic pathway (in blue), threonine biosynthetic pathway (in green), and designed pentanol biosynthetic pathway (*Right*). Pentanol synthesis starts from condensation of one acetyl-CoA with one propionyl-CoA, instead of two acetyl-CoA molecules, to establish a five-carbon skeleton.

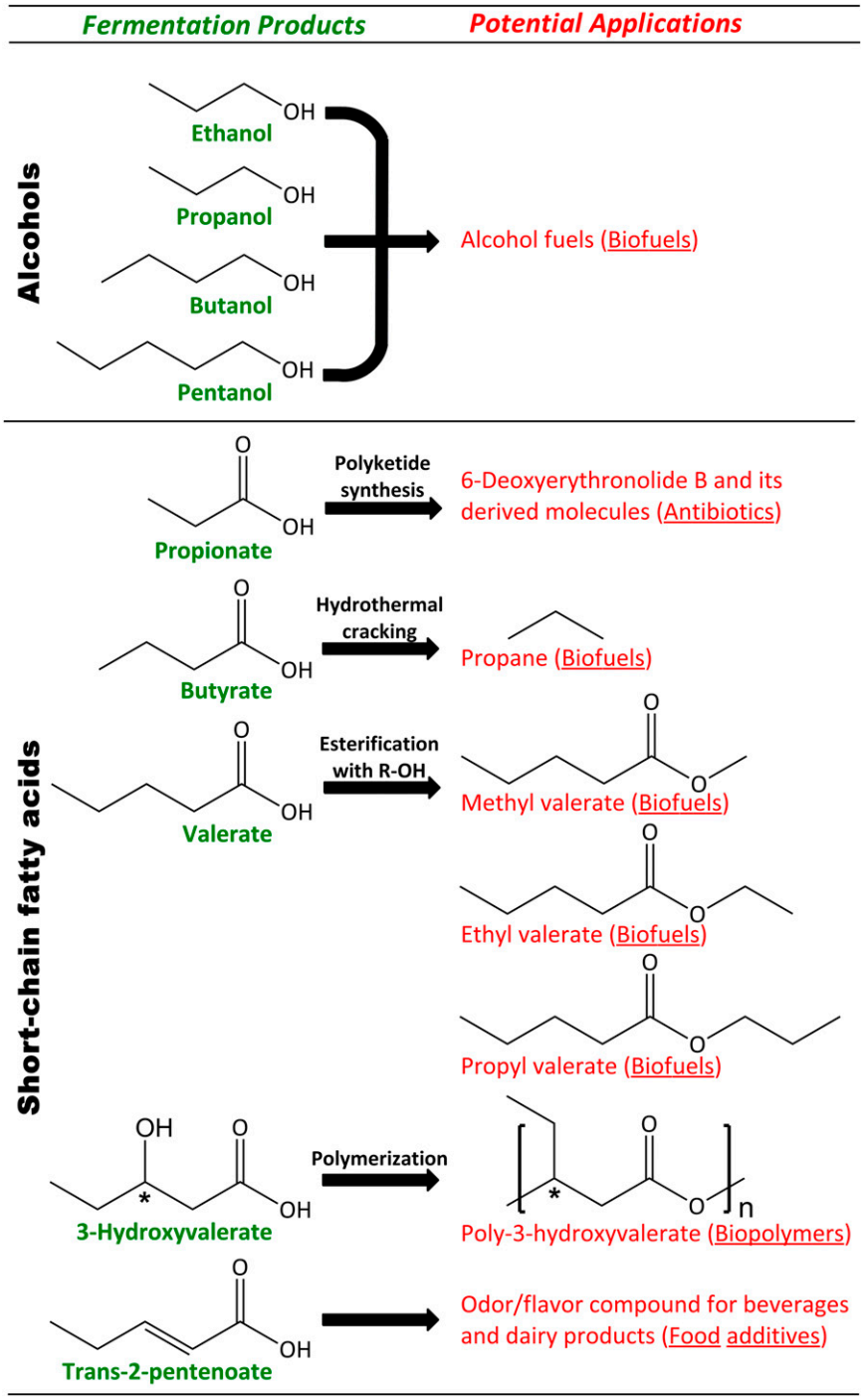

Fig. S2. Applications of various fermentation products synthesized from recombinant *Escherichia coli* strains carrying different combinations of pentanol pathway and CoA-activation/removing toolkit enzymes.

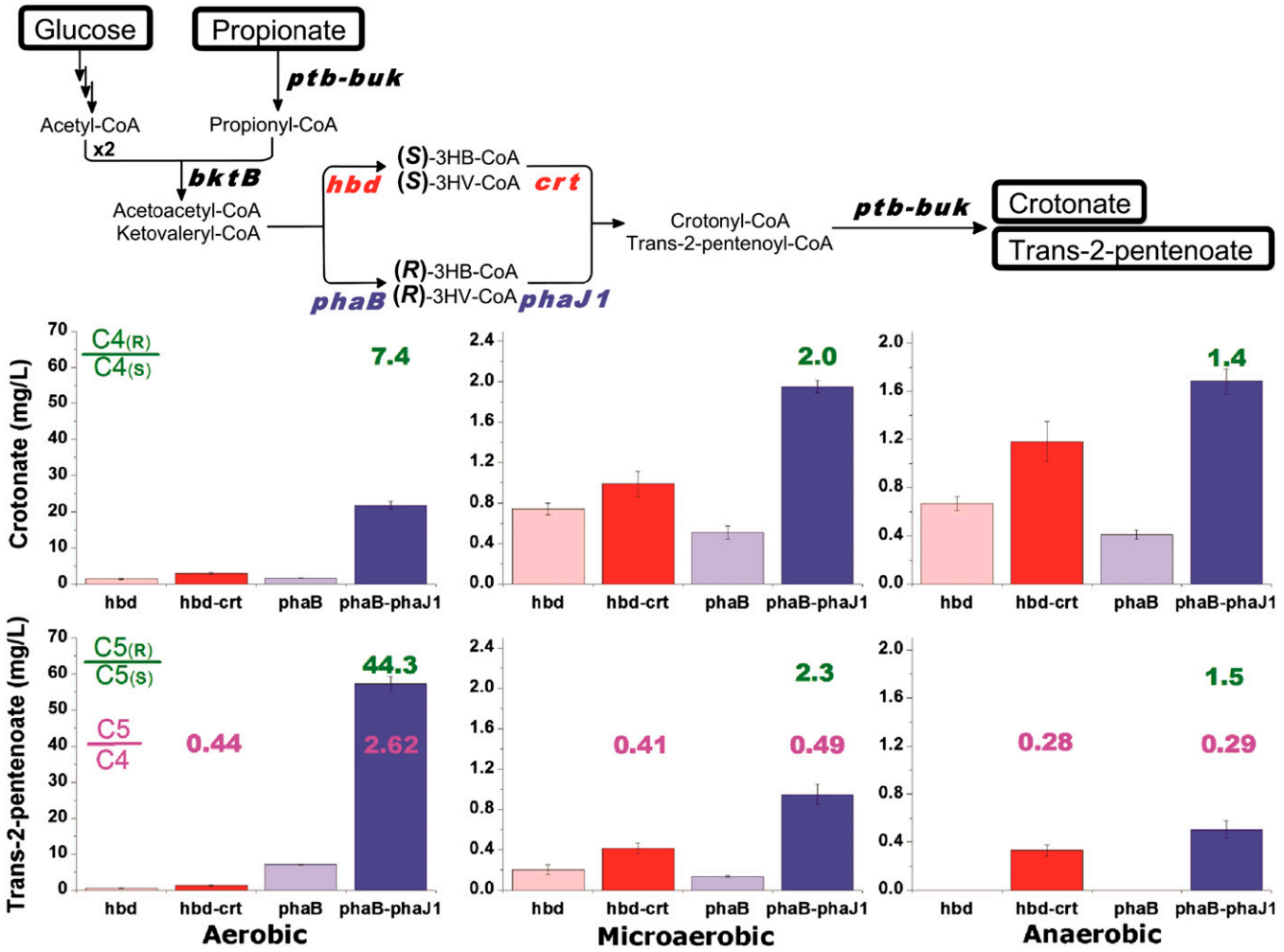

Fig. S3. Schematic of trans-2-pentenoate biosynthetic pathway (*Upper*) and titers of products synthesized by recombinant *E. coli* grown under various conditions (*Lower*). All constructs contain *ptb-buk* and *bktB* in addition to the genes indicated under each bar. The symbols of C4 and C5 denote crotonate and trans-2-pentenoate, respectively. Ratios of titers from *phaB-phaJ1* constructs to titers from *hbd-crt* constructs are shown in green and ratios of trans-2-pentenoate titers to crotonate titers are shown in pink. Cells were grown in TB supplemented with 10 g/L glucose and 20 mM propionate, and incubated at 30 °C for 24 h. For the ratios of product titers from *phaB-phaJ1* constructs to those from *hbd-crt*, a value larger than 1 suggests that the *R*-pathway outperforms the *S*-pathway, which was the case under aerobic conditions. On the other hand, the ratio was close to one under anaerobic conditions, suggesting that the difference between the *R*- and *S*-pathway became smaller. For the ratios of tran-2-penenote titers to crotonate titers, the values also dropped when culture condition changes from aerobic to anaerobic. The difference in the two ratios between the *R*- and *S*- pathway implicates a correlation between oxygen availability and *R*- and *S*-pathway activities, to explain which, a hypothesis is proposed in Fig. S4.

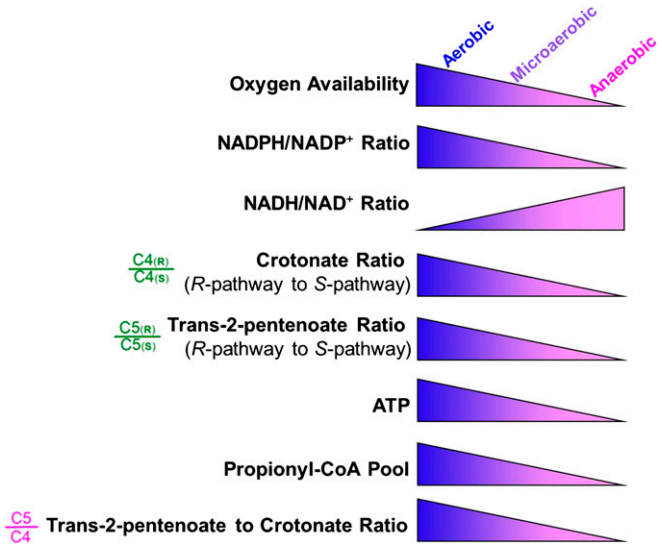

Fig. S4. Schematic representation of correlations between dissolved oxygen and various variables (cofactor ratios, ATP, and observed product ratios). The results of trans-2-pentenoate synthesis from glucose and glycerol under aerobic, microaerobic, and anaerobic culture conditions suggest that there may exist a correlation between oxygen availability and *R*- and *S*-pathway activities, to explain which a hypothesis was proposed. As generally known, the NADPH/NADP$^+$ ratio is positively correlated with DOT (dissolved oxygen tension) but the NADH/NAD$^+$ ratio is inversely correlated with DOT, so we would expect the NADPH-dependent *R*-pathway to outperform the NADH-dependent *S*-pathway under aerobic conditions, resulting in larger crotonate ratios (*R*-pathway to *S*-pathway) and trans-2-pentenoate ratios (*R*-pathway to *S*-pathway) (Fig. S3). Under anaerobic conditions, the trend of cofactor ratios reverses, and the difference in performance between the two pathways should become smaller, which is consistent with our observations. In addition, we suspected that the activation of propionate is also affected by DOT as its activation by Ptb-Buk requires ATP, the amount of which is positively correlated with DOT. Thus, a larger propionyl-CoA pool could be expected under the aerobic conditions, thus favoring the condensation reaction of acetyl-CoA with propionyl-CoA, and consequently resulting in larger trans-2-pentenoate to crotonate ratios (Fig. S3). These observations gave insights into optimization of culture conditions, motivating us to profile various headspace to culture volume ratios for production of butanol (Fig. S8).

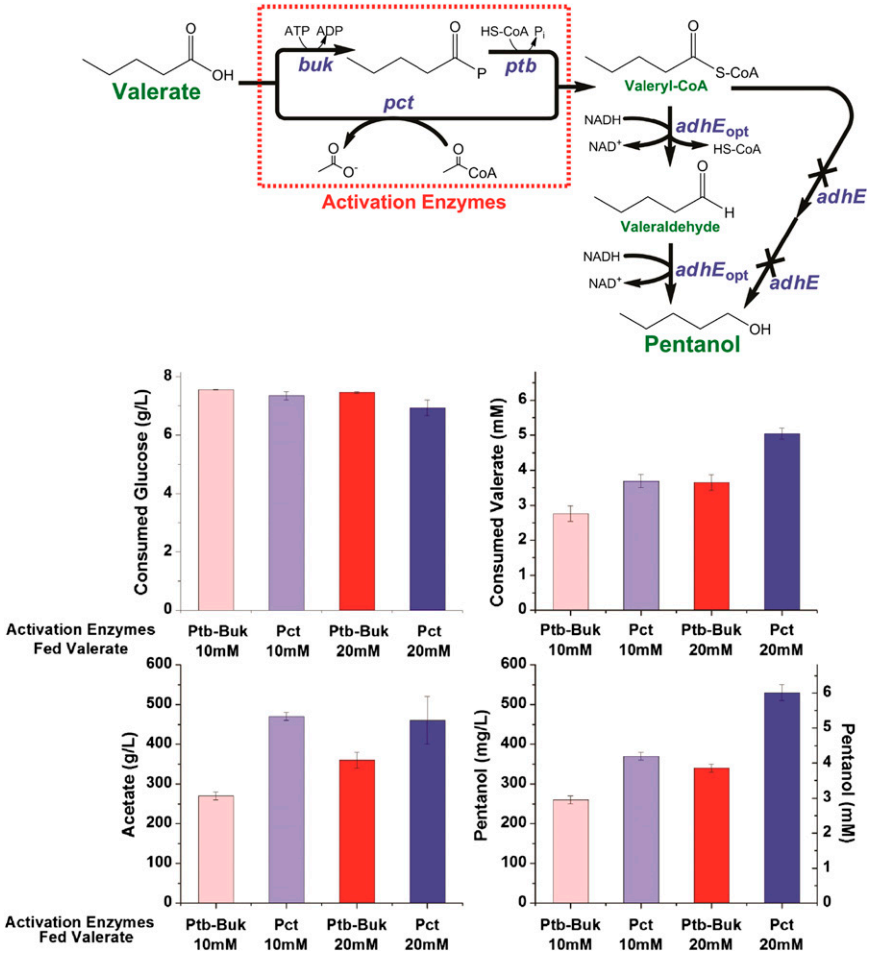

Fig. S5. Schematic diagram of pentanol synthesis from valerate and titers of substrates consumed and products synthesized by recombinant *E. coli*. Two activators, including Ptb-Buk and Pct, and two feed concentrations of valerate, were compared. The $adhE_{opt}$ gene was overexpressed in all constructs. Stains using Pct as the CoA-activator were found to consume more valerate and produce more pentanol compared with stains using Ptb-Buk as CoA-activator. Pentanol titers were further boosted when the valerate substrate concentration was increased from 10 mM to 20 mM. Overall, the results suggest that the AdhE enzyme, expressed from the codon-optimized $adhE_{opt}$, was able to catalyze the reaction of valeryl-CoA to pentanol.

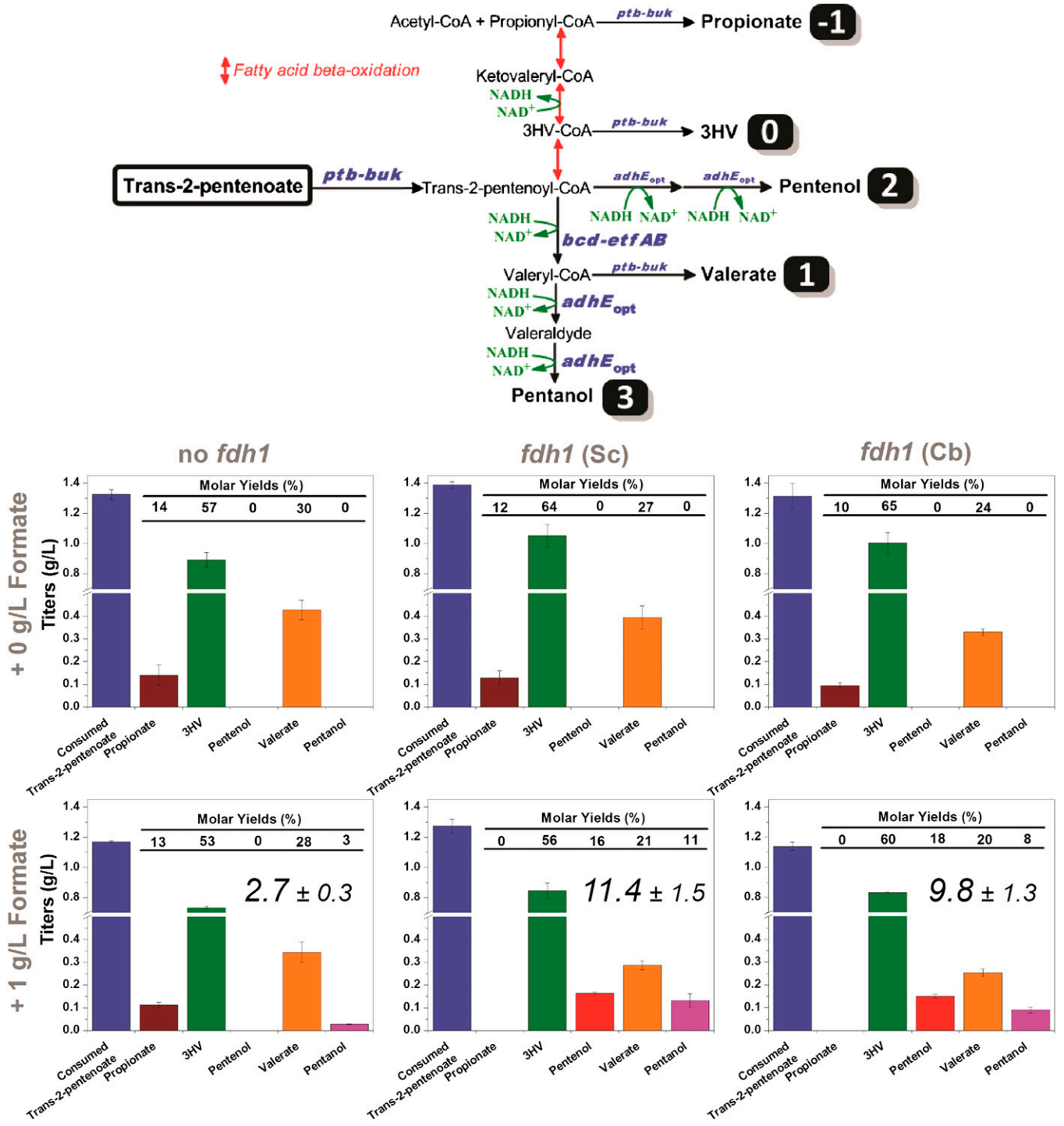

Fig. S6. Schematic diagram of pentanol synthesis from trans-2-pentenoate and titers of products resulting from the feeding of trans-2-pentenoate. All relevant products coming from trans-2-petenoate are shown. Genes of *ptb-buk*, *bcd-etfAB*, and $adhE_{opt}$ were overexpressed. Two formate dehydrogenases (encoded by *fdh1* with codon-optimization) from *Saccharomyces cerevisiae* and *Candida boidinii* were overexpressed to increase NADH availability. The effect of supplementation with 1 g/L formate was also compared. To quantify the effect of overexpression of *fdh1*, one number was assigned to each product based on its relative redox state, for example, "2" for pentenol synthesized from trans-2-pentenoyl-CoA requires 2 mol of NADH, and "−1" for propionate synthesized from trans-2-pentenoyl-CoA generates 1 mol of NADH. Next, we calculated the total NADH used for product formation, which is the summation of products of multiplying the relative redox value by the product titer. The calculated total NADH used for product formation is shown within each of the bottom three plots. Clearly, the overexpression of *fdh1* with supplementation of formate increased the NADH availability within the cells as the total NADH used for product formation increased from 2.7 in the no-*fdh1* control to 11.4 and 9.8 in cells expressing *S. cerevisiae fdh1* and *C. boidinii fdh1*, respectively. Additionally, the observation of production of valerate and pentanol in the *bcd-etfAB* containing strain suggest that the Bcd enzyme used in the bottom pentanol pathway can transform trans-2-pentenoyl-CoA, a five-carbon substrate, to valeryl-CoA.

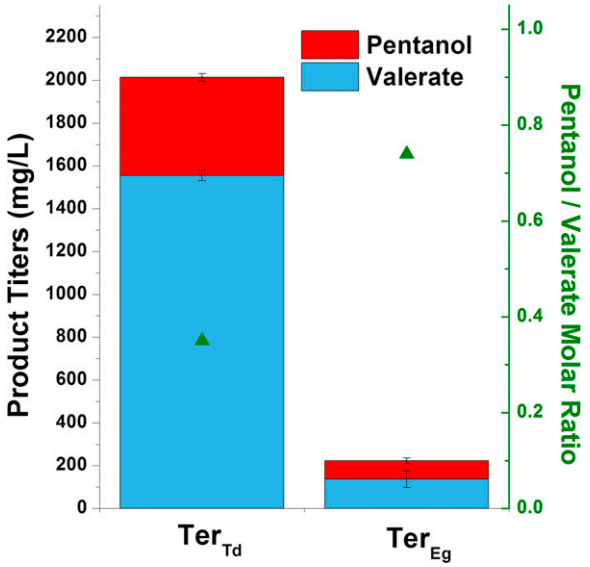

Fig. S7. Comparison of the two Ter enzymes from *Treponema denticola* and *Euglena gracilis* on pentanol synthesis. The Ter_{Td} enzyme obviously outperformed the Ter_{Eg} enzyme in converting trans-2-pentenoyl-CoA to valeryl-CoA, resulting in more valerate and pentanol despite its incapability of catalyzing hexanoyl-CoA, a C6 substrate, based on a reported in vitro enzyme assay result (1). The $fdh1_{Sc}$ gene was overexpressed in both strains along with supplementation of 1 g/L formate.

1. Tucci S, Martin W (2007) A novel prokaryotic trans-2-enoyl-CoA reductase from the spirochete *Treponema denticola*. *FEBS Lett* 581(8):1561–1566.

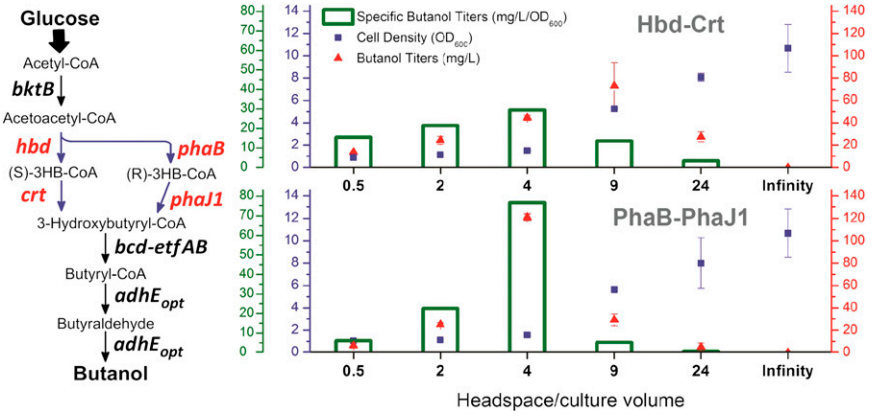

Fig. S8. Butanol synthesis from glucose via newly constructed pentanol pathways. This figure shows butanol titers, specific titers, and cell densities from cultures of recombinant *E. coli* containing the pentanol pathways. Cells were grown under various culture conditions with different ratios of headspace to culture volume for 48 h. Two routes, including the *hbd-crt* route (*Upper*, strain Pal5) and the *phaB-phaJ1* (*Lower*, strain Pal6) route, were compared. In general, strains containing either *R*- or *S*- pentanol biosynthetic pathway produced butanol, achieving the highest butanol specific titers at a headspace to culture volume ratio of 4.

Table S1. Comparison of physical-chemical properties of various biofuels and gasoline

Fuels	Air-fuel ratio	Vapor pressure (psi)	Energy density (MJ/kg)	Fits current infrastructure?
Gasoline	14.6	0.1–30	42.7	Yes
Ethanol	9.0	1.1	29.7	No
Butanol	11.2	0.077	36.1	Yes
Isobutanol	11.2	0.17	36.1	Yes
Pentanol	12.5	0.039	37.7	Yes

Although ethanol represents an initial success as a biofuel because of its high production yield and efficiency, it does not compare favorably to gasoline. Ethanol has a lower energy density (~34% less energy per unit volume than gasoline, resulting in a 34% reduction in miles per gallon), a low vapor pressure, and a high hygroscopicity, possibly leading to corrosion in pipelines and engines. Furthermore, ethanol raises the vapor pressure of the mixture when blended to gasoline, although this is partially offset by an increase in octane number. In contrast, advanced biofuels, including butanol, isobutanol, and pentanol, have better physical-chemical properties, such as higher energy densities, low hygroscopicities as well as lower vapor pressure for gasoline blends. Although the octane number of l-butanol is slightly less than gasoline, branched-chain isomers, such as isobutanol, have higher octane numbers, allowing for more flexibility in fuel design. Furthermore, as carbon length increases, the amount of air needed to combust unit amount of fuel also increases. Because standard gasoline engines can only adjust the air-fuel ratio to accommodate variations in the fuel within certain limits, the closer to 14.6 the air-fuel ratio of the fuels, the better the engine's efficiency. Therefore, long-chain alcohols are preferable fuel alternatives. Perry's handbook (1) and www2.dupont.com/BioFuel/en_US/index.html.

1. Perry R, Green D (2007) *Perry's Chemical Engineers' Handbook* (McGraw-Hill, New York).

Table S2. List of strains and plasmids used in this work

Strain or plasmid	Relevant genotype	Ref.
Strain		
DH10B	*F⁻ mcrA Δ(mrr-hsdRMS-mcrBC) ψ80lacZΔM15 ΔlacX74 recA1 endA1 araD139Δ (ara, leu)7697 galU galK λ⁻ rpsL nupG*	Invitrogen
ElectroTen-Blue	*Δ (mcrA)183 Δ (mcrCB-hsdSMR-mrr)173 endA1 supE44 thi-1 recA1 gyrA96 relA1 lac Kan^r [F′proAB lacI^qZΔM15 Tn10 (Tet^r)]*	Stratagene
BL21Star(DE3)	*F⁻ ompT hsdSB (rB⁻ mB⁻) gal dcm rne131 (DE3)*	Invitrogen
Module 3		
BL1	pCDF/ptb-buk + pACYC/adhE	Present study
BL2	pCDF/ptb-buk + pACYC/adhE$_{opt}$	Present study
BL3	pCDF/pct + pACYC/adhE	Present study
BL4	pCDF/pct + pACYC/adhE$_{opt}$	Present study
BL5	pCDF/pct + pACYC/yiaY	Present study
BL6	pET/bcd-etfAB/adhE$_{opt}$ + pCDF/ptb-buk	Present study
BL7	pET/bcd-etfAB/adhE$_{opt}$ + pCDF/ptb-buk/fdh1$_{Sc}$	Present study
BL8	pET/bcd-etfAB/adhE$_{opt}$ + pCDF/ptb-buk/fdh1$_{Cb}$	Present study
BL9	pET/Ter$_{Td}$/adhE$_{opt}$ + pCDF/ptb-buk/fdh1$_{Sc}$	Present study
BL10	pET/Ter$_{Eg}$/adhE$_{opt}$ + pCDF/ptb-buk/fdh1$_{Sc}$	Present study
BL11	pET/Ter$_{Td}$/adhE$_{opt}$ + pCDF/ptb-buk/fdh1$_{Sc}$+ pACYCDuet-1	Present study
BL12	pET/Ter$_{Td}$/adhE$_{opt}$ + pCDF/ptb-buk/fdh1$_{Sc}$+ pACYC/aceEF-lpd$_{101}$	Present study
MG1655	F⁻ λ⁻ *ilvG- rfb-50 rph-1*	ATCC 700926
Pal(DE3)	MG1655(DE3 Δ*pta* Δ*adhE* Δ*ldhA*)	(1)
Module 2		
Pal1	pET/bktB/hbd + pCDF/ptb-buk/crt	Present study
Pal2	pET/bktB/hbd + pCDF/ptb-buk	Present study
Pal3	pET/bktB/phaB + pCDF/ptb-buk/phaJ1	Present study
Pal4	pET/bktB/phaB + pCDF/ptb-buk	Present study
Pal5	pET/bcd-etfAB/bktB + pCDF/crt/hbd + pACYC/adhE$_{opt}$	Present study
Pal6	pET/bcd-etfAB/bktB + pCDF/phaJ1/phaB + pACYC/adhE$_{opt}$	Present study
Module 2+3		
Pal7	pETDuet-1 + pCDFDuet-1 + pACYCDuet-1	Present study
Pal8	pET/bcd-etfAB/bktB/pct + pCDF/crt/hbd + pACYC/fdh1$_{Sc}$/adhE$_{opt}$	Present study
Pal9	pET/bcd-etfAB/bktB/pct + pCDF/crt/hbd + pACYC/fdh1$_{Cb}$/adhE$_{opt}$	Present study
Pal10	pET/Ter$_{Td}$/bktB/pct + pCDF/crt/hbd + pACYC/fdh1$_{Sc}$/adhE$_{opt}$	Present study
Pal11	pET/Ter$_{Td}$/bktB/pct + pCDF/crt/hbd + pACYC/fdh1$_{Sc}$/aceEF-lpd$_{101}$/adhE$_{opt}$	Present study
Pal12	pET/Ter$_{Td}$/bktB/pct + pCDF/crt/hbd + pACYC/fdh1$_{Sc}$/aceEF-lpd$_{101}$	Present study
Pal13	pET/bcd-etfAB/bktB/pct + pCDF/phaJ1/phaB + pACYC/fdh1$_{Sc}$/adhE$_{opt}$	Present study
Pal14	pET/bcd-etfAB/bktB/pct + pCDF/phaJ1/phaB + pACYC/fdh1$_{Cb}$/adhE$_{opt}$	Present study
Pal15	pET/Ter$_{Td}$/bktB/pct + pCDF/phaJ1/phaB + pACYC/fdh1$_{Sc}$/adhE$_{opt}$	Present study
Pal16	pET/Ter$_{Td}$/bktB/pct + pCDF/phaJ1/phaB + pACYC/fdh1$_{Sc}$/aceEF-lpd$_{101}$/adhE$_{opt}$	Present study
Module 1+2+3		
Pal17	pET/bcd-etfAB/bktB + pCDF/crt/hbd + pACYC/adhE$_{opt}$ + pCOLA/thrA^{fr}BC/ilvA^{fr}	Present study
Pal18	pET/bcd-etfAB/bktB + pCDF/crt/hbd + pACYC/fdh1$_{Sc}$/adhE$_{opt}$+ pCOLA/thrA^{fr}BC/ilvA^{fr}	Present study
Pal19	pET/bcd-etfAB/bktB + pCDF/crt/hbd + pACYC/fdh1$_{Cb}$/adhE$_{opt}$+ pCOLA/thrA^{fr}BC/ilvA^{fr}	Present study
Pal20	pET/bcd-etfAB/bktB + pCDF/phaJ1/phaB + pACYC/adhE$_{opt}$+ pCOLA/thrA^{fr}BC/ilvA^{fr}	Present study
Pal21	pET/bcd-etfAB/bktB + pCDF/phaJ1/phaB + pACYC/fdh1$_{Sc}$/adhE$_{opt}$+ pCOLA/thrA^{fr}BC/ilvA^{fr}	Present study
Pal22	pET/bcd-etfAB/bktB + pCDF/phaJ1/phaB + pACYC/fdh1$_{Cb}$/adhE$_{opt}$+ pCOLA/thrA^{fr}BC/ilvA^{fr}	Present study
Pal23	pET/Ter$_{Td}$/bktB + pCDF/crt/hbd + pACYC/fdh1$_{Sc}$/aceEF-lpd$_{101}$/adhE$_{opt}$ + pCOLA/thrA^{fr}BC/ilvA^{fr}	Present study
Pal24	pET/Ter$_{Td}$/bktB + pCDF/crt/hbd + pACYC/fdh1$_{Sc}$/aceEF-lpd$_{101}$ + pCOLA/thrA^{fr}BC/ilvA^{fr}	Present study
Pal25	pCDF/tesB + pCOLA/thrA^{fr}BC/ilvA^{fr}	Present study
Pal(DE3 Δ*mdh*)	MG1655(DE3 Δ*pta* Δ*ldhA* Δ*adhE* Δ*mdh*)	
Palm1	pET/Ter$_{Td}$/bktB + pCDF/crt/hbd + pACYC/fdh1$_{Sc}$/ aceEF-lpd$_{101}$/adhE$_{opt}$ + pCOLA/thrA^{fr}BC/ilvA^{fr}	Present study
Pal(DE3 Δ*tesB*)	MG1655(DE3 Δ*pta* Δ*ldhA* Δ*adhE* Δ*tesB*)	
Palt1	pET/Ter$_{Td}$/bktB + pCDF/crt/hbd + pACYC/fdh1$_{Sc}$/ aceEF-lpd$_{101}$/adhE$_{opt}$ + pCOLA/thrA^{fr}BC/ilvA^{fr}	Present study
Plasmid		
pETDuet-1	ColE1(pBR322) *ori*, *lacI*, T7*lac*, Amp^{R}	Novagen
pET/bcd-etfAB/bktB	pETDuet-1 harboring *bcd-etfAB* operon from *Clostridium acetobutylicum* ATCC 824, and *bktB* from *Cupriavidus necator* (formerly known as *Ralstonia eutropha*) H16	Present study
pET/bcd-etfAB/bktB/pct	pETDuet-1 harboring *bcd-etfAB* operon from *C. acetobutylicum* ATCC 824, *bktB* from *C. necator* H16,and *pct* from *Megasphaera elsdenii*	Present study
pET/bcd-etfAB/adhE$_{opt}$	pETDuet-1 harboring *bcd-etfAB* operon and codon-optimized *adhE*$_{opt}$ from *C. acetobutylicum* ATCC 824	Present study

Table S2. Cont.

Strain or plasmid	Relevant genotype	Ref.
pET/Ter_{Td}/bktB	pETDuet-1 harboring *ter* from *T. denticola*, and *bktB* from *C. necator* H16	Present study
pET/Ter_{Td}/bktB/pct	pETDuet-1 harboring *ter* from *T. denticola*, *bktB* from *C. necator* H16, and *pct* from *M. elsdenii*	Present study
pET/Ter_{Td}/$adhE_{opt}$	pETDuet-1 harboring *ter* from *T. denticola*, and codon-optimized $adhE_{opt}$ from *C. acetobutylicum* ATCC 824	Present study
pET/Ter_{Eg}/$adhE_{opt}$	pETDuet-1 harboring *ter* from *E. gracilis*, and codon-optimized $adhE_{opt}$ from *C. acetobutylicum* ATCC 824	Present study
pET/bktB/hbd	pETDuet-1 harboring *bktB* from *C. necator* H16, and *hbd* from *C. acetobutylicum* ATCC 824	(2)
pET/bktB/phaB	pETDuet-1 harboring *bktB* and *pha*B from *C. necator* H16	(2)
pCDFDuet-1	CloDF13 *ori*, *lacI,* T7*lac*, $Strep^R$	Novagen
pCDF/crt/hbd	pCDFDuet-1 harboring *crt* and *hbd* from *C. acetobutylicum* ATCC 824	Present study
pCDF/phaJ1/phaB	pCDFDuet-1 harboring *phaJ1* from *P. aeruginosa, and pha*B from *C. necator* H16	Present study
pCDF/ptb-buk	pCDFDuet-1 harboring *ptb-buk* operon from *C. acetobutylicum* ATCC 824	(3)
pCDF/ptb-buk/$fdh1_{Sc}$	pCDFDuet-1 harboring *ptb-buk* operon from *C. acetobutylicum* ATCC 824, and codon-optimized *fdh1* from *S. cerevisia*e	Present study
pCDF/ptb-buk/$fdh1_{Cb}$	pCDFDuet-1 harboring *ptb-buk* operon from *C. acetobutylicum* ATCC 824, and codon-optimized *fdh1* from *C. boidinii*	Present study
pCDF/ptb-buk/crt	pCDFDuet-1 harboring *ptb-buk* operon and *crt* from *C. acetobutylicum* ATCC 824	Present study
pCDF /ptb-buk/phaJ1	pCDFDuet-1 harboring *ptb-buk* operon from *C. acetobutylicum* ATCC 824, and *phaJ1* from *P. aeruginosa*	Present study
pCDF/pct	pCDFDuet-1 harboring *pct* from *M. elsdenii*	(4)
pCDF/tesB	pCDFDuet-1 harboring *tesB* from *E. coli* MG1655	(2)
pACYCDuet-1	P15A *ori*, *lacI,* T7*lac,* Cm^R	Novagen
pACYC/adhE	pACYCDuet-1 harboring *adhE* from *C. acetobutylicum* ATCC 824	(3)
pACYC/$adhE_{opt}$	pACYCDuet-1 harboring codon-optimized $adhE_{opt}$ from *C. acetobutylicum* ATCC 824	Present study
pACYC/yiaY	pACYCDuet-1 harboring *yiaY* from *E. coli* MG1655	Present study
pACYC/aceEF-lpd_{101}	pACYCDuet-1 harboring *aceEF-*lpd_{101} operon from *E. coli* SE2378	Present study
pACYC /$fdh1_{Sc}$/$adhE_{opt}$	pACYCDuet-1 harboring codon-optimized *fdh1* from *S. cerevisia*e, and codon-optimized $adhE_{opt}$ from *C. acetobutylicum* ATCC 824	Present study
pACYC /$fdh1_{Sc}$/aceEF-lpd_{101}/$adhE_{opt}$	pACYCDuet-1 harboring codon-optimized *fdh1* from *S. cerevisia*e, *aceEF-*lpd_{101} operon from *E. coli* SE2378 and codon-optimized $adhE_{opt}$ from *C. acetobutylicum* ATCC 824	Present study
pACYC /$fdh1_{Sc}$/aceEF-lpd_{101}	pACYCDuet-1 harboring codon-optimized *fdh1* from *S. cerevisia*e, and *aceEF-*lpd_{101} operon from *E. coli* SE2378	Present study
pACYC /$fdh1_{Cb}$/$adhE_{opt}$	pACYCDuet-1 harboring codon-optimized *fdh1* from *C. boidinii*, and codon-optimized $adhE_{opt}$ from *C. acetobutylicum* ATCC 824	Present study
pCOLADuet-1	COLA *ori*, *lacI,* T7*lac*, Kan^R	Novagen
pCOLA/$thrA^{fr}$BC/$ilvA^{fr}$	pCOLADuet-1 harboring $thrA^{G1297A}BC$ operon from *E. coli* ATCC 21277, and $ilvA^{fr}$ from *C. glutamicum* ATCC 13032	(5)

1. Fischer CR, Tseng HC, Tai M, Prather KL, Stephanopoulos G (2010) Assessment of heterologous butyrate and butanol pathway activity by measurement of intracellular pathway intermediates in recombinant *Escherichia coli*. *Appl Microbiol Biotechnol* 88(1):265–275.
2. Tseng H-C, Martin CH, Nielsen DR, Prather KLJ (2009) Metabolic engineering of *Escherichia coli* for the enhanced production of (R)- and (S)-3-hydroxybutyrate. *Appl Environ Microbiol* 75(10):3137–3145.
3. Nielsen DR, et al. (2009) Engineering alternative butanol production platforms in heterologous bacteria. *Metab Eng* 11(4-5):262–273.
4. Martin CH (2010) Development of metabolic pathways for the biosynthesis of hydroxyacids and lactones. PhD dissertation (Massachusetts Institute of Technology, Cambridge, MA). Available at http://hdl.handle.net/1721.1/57867.
5. Tseng HC, Harwell CL, Martin CH, Prather KL (2010) Biosynthesis of chiral 3-hydroxyvalerate from single propionate-unrelated carbon sources in metabolically engineered *E. coli*. *Microb Cell Fact* 9:96.

Table S3. List of DNA oligonucleotides used in this work

Primer	Sequence 5′→3′	Source
crt-FP-BamHI	ATAGGATCCAGGAGGATTAGTCATGGAAC	Sigma-Genosys
crt-RP-NotI	ATAGCGGCCGCAAACTTACCTCCTATCTATTTTTG	Sigma-Genosys
crt-FP-MfeI	TAACAATTGGGAGGATTAGTCATGG	Sigma-Genosys
crt-RP-XhoI	ATTCTCGAGTACCTCCTATCTATTTTTG	Sigma-Genosys
phaJ1-FP-BamHI	ATAGGATCCAGGGGAGAGAACATGAGCCAGGTCCAGAAC	Sigma-Genosys
phaJ1-RP-NotI	ATAGCGGCCGCTCAGCCGATGCTGATCGG	Sigma-Genosys
phaJ1-FP-NdeI	ATACATATGAGGGGAGAGAACATGAGCCAGGTCCAGAAC	Sigma-Genosys
phaJ1-RP-AvrII	ATACCTAGGTCAGCCGATGCTGATCGG	Sigma-Genosys
bcd-FP-BamHI	ATTAGGATCCAAGGAGAGTTTATATGGATTTTAATTTAAC	Sigma-Genosys
bcd-RP-NotI	ATTAGCGGCCGCATTTATCTTAATTATTAGCAGC	Sigma-Genosys
$fdh1_{Sc}$-FP-BamHI	ATAGGATCCAGGGGATATCATATGATGTCCAAAGGCAAAG	Sigma-Genosys
$fdh1_{Sc}$-RP-SalI	ATAGTCGACCCTAGGTTATTTTTTCTGACCATACG	Sigma-Genosys
$fdh1_{Cb}$-FP-BamHI	ATAGGATCCAGGGGATATCATATGATGAAAATCGTGCTGG	Sigma-Genosys
$fdh1_{Cb}$-RP-SalI	ATAGTCGACCCTAGGTCATTTTTTGTCGTGTTT	Sigma-Genosys
pct-FP-XhoI	ATACTCGAGAGGGGAGAATTCATGAGAAAAGTAGAAATC	Sigma-Genosys
pct-RP-AvrII	ATACCTAGGACCTGCAGTTATTTTTTCAGT	Sigma-Genosys
bktB-FP-EcoRI	ATAGAATTCAGGGGAAAAGTCATGACGCGTGAAGTGG	Sigma-Genosys
bktB-RP-HindIII	ATAAAGCTTAACCTCAGATACGCTCGAAGATGG	Sigma-Genosys
aceE-FP-SalI	ATTAGTCGACAAGGAGATATTATATGTCAGAACGTTTCCCAAATGACG	Sigma-Genosys
lpd101-RP-NotI	ATTAGCGGCCGCTTACTTCTTCTTCGCTTTCGGGTTC	Sigma-Genosys
yiaY-FP-AatII	ATTAGACGTCAAGGAGATATTATATGGCAGCTTCAACGTTCTT	Sigma-Genosys
yiaY-RP-AvrII	ATTACCTAGGCCGTTGTGGAAATGATGATTAC	Sigma-Genosys
hbd-FP-NdeI	ATTCATATGAAAAAGGTATGTGTTATAGG	Sigma-Genosys
hbd-RP-XbaI	ATTTCTAGAACTTATTTTGAATAATCGTAG	Sigma-Genosys
phaB-FP-MfeI	ATTCAATTGACGAAGCCAATCAAGGAG	Sigma-Genosys
phaB-RP-AvrII	ATTCCTAGGGGTCAGCCCATATGCAG	Sigma-Genosys
C-FP-tesB (for colony PCR)	TTTCTCCTTATTATCAATGCACC	Sigma-Genosys
C-RP-tesB (for colony PCR)	CATTTATCGGCTACAAATTGG	Sigma-Genosys
C-FP-mdh (for colony PCR)	GCGACTGTTAATTACGTAAGTTAGG	Sigma-Genosys
C-RP-mdh (for colony PCR)	CCCTGTAGTAGTGATGCGTG	Sigma-Genosys

Restriction sites used for cloning are underlined. Primer names correspond to the name of the gene that the primer amplifies, whether the primer is the forward primer (FP) or reverse primer (RP) of that gene, and the restriction site incorporated into the primer sequence for cloning.